The C-terminal kinesin motor KIFC1 may participate in nuclear reshaping and flagellum formation during spermiogenesis of *Larimichthys crocea*

Dan-Dan Zhang · Xin-Ming Gao · Yong-Qiang Zhao · Cong-Cong Hou · Jun-Quan Zhu

Abstract Spermatogenesis is a highly ordered process in the differentiation of male germ cells. Nuclear morphogenesis is one of the most fundamental cellular transformations to take place during spermatogenesis. These striking transformations from spermatogonia to spermatozoa are a result of phase-specific adaption of the cytoskeleton and its association with molecular motor proteins. KIFC1 is a C-terminal kinesin motor protein that plays an essential role in acrosome formation and nuclear reshaping during spermiogenesis in mammals. To explore its functions during the same process in *Larimichthys crocea*, we cloned and characterized the cDNA of a mammalian KIFC1 homolog (termed *lc*-KIFC1) from the total RNA of the testis. The 2481 bp complete *lc*-KIFC1 cDNA contained a 53 bp 5′ untranslated region, a 535 bp 3′ untranslated region, and a 1893 bp open reading frame that encoded a special protein of 630 amino acids. The predicted *lc*-KIFC1 protein possesses a divergent tail region, stalk region, and conserved carboxyl motor region. Protein alignment demonstrated that *lc*-KIFC1 had 73.2, 49.8, 49.3, 54.6, 56.5, 53.1, and 52.1% identity with its homologs in *Danio rerio*, *Eriocheir sinensis*, *Octopus tankahkeei*, *Gallus gallus*, *Xenopus laevis*, *Mus musculus*, and *Homo sapiens*, respectively. Tissue expression analysis revealed that *lc-kifc1* mRNA was mainly expressed in the testis. The trend of *lc-kifc1* mRNA expression at different growth stages of the testis showed that the expression increased first and then decreased, in the stage IV of testis, its expression quantity achieved the highest level. In situ hybridization and immunofluorescence results showed that KIFC1 was localized around the nucleus in early spermatids. As spermatid development progressed, the signals increased substantially. These signals peaked and were concentrated at one end of the nucleus when the spermatids began to undergo dramatic changes. In the mature sperm, the signal for KIFC1 gradually became weak and was mainly localized in the tail. In summary, evaluation of the expression pattern for *lc*-KIFC1 at specific stages of spermiogenesis has shed light on the potential functions of this motor protein in major cytological transformations. In addition, this study may provide a model for researching the molecular mechanisms involved in spermatogenesis in other teleost species, which will lead to a better understanding of the teleost fertilization process.

Keywords Spermiogenesis · *lc*-KIFC1 · *Larimichthys crocea* · Nuclear reshaping · Flagellum formation

Abbreviations

KIFC1	C-terminal kinesin C1
KHCs	Kinesin heave chains
KLCs	Kinesin light chains
AFS	Acroframosome
LCx	Lamellar complex
CTK2	C-terminal kinesin-2

D.-D. Zhang · X.-M. Gao · Y.-Q. Zhao · C.-C. Hou (✉) · J.-Q. Zhu (✉)
Key Laboratory of Applied Marine Biotechnology by the Ministry of Education, School of Marine Sciences, Ningbo University, Ningbo, Zhejiang 315211, China
e-mail: houcongcong@nbu.edu.cn
e-mail: zhujunquan@nbu.edu.cn

qRT-PCR	Real-time quantitative polymerase chain reaction
RACE	Rapid amplification of cDNA ends
UTR	Untranslated region
ORF	Open reading frame
ISH	In situ hybridization
IF	Immunofluorescence
O.C.T	Optimum cutting temperature
PBS	Phosphate-buffered saline
DEPC	Diethyl pyrocarbonate
SSC	Standard sodium chloride
DIG	Digoxigenin
PFA	Paraformaldehyde
BSA	Albumin from bovine serum
SD	Standard deviation

Introduction

Spermatogenesis is a complex developmental process orchestrated by intricate signaling pathways, which generates a large number of mature functional sperm in the testis that subsequently participate in fertilization (Oakberg 1956; Fawcett 1975; He et al. 2009). Spermatogenesis can be divided into three main phases beginning with the mitotic proliferation of spermatogonia that provides a pool of stem cells, after which spermatocytes undergo meiotic division to produce haploid round spermatids. The most prominent structural, functional, and morphological transformations occur during the last phase of spermatogenesis, wherein these haploid germ cells undergo essential changes including biogenesis of the lysosome-like acrosome, condensation and elongation of the sperm head, and emergence of the motile flagellum, culminating with the release of viable sperm into the lumen of the seminiferous tubules (Hess and Renato 2008; Hermo et al. 2010a, b). These morphological changes are essentially the result of a strict regulation of stage-specific gene expression (Kimmins et al. 2004; Lui and Cheng 2008), which is demonstrated partially in the form of spermatid-specific modification of the cytoskeleton and involvement of related molecular motor proteins (Zou et al. 2002; Wang and Sperry 2008).

Kinesin is a superfamily containing a group of motor proteins of which the most significant function is directing intracellular transportation of various cargoes including membranous organelles, vesicles, lipid drops,

pigments, protein complexes, mRNAs, and chromosomes moving along microtubules via ATP hydrolysis to different destinations (Hirokawa and Takemura 2004; Kikkawa 2008). A typical kinesin is mainly composed of three domains: two large globular head motor domains that have microtubule and ATP-binding sites, a central coiled stalk domain that is used to stabilize the configuration of the protein, and the tail domain, which is used to transport various cargos (Hirokawa and Noda 2008). Based on the location of the motor domain, the kinesin superfamily is classified into three major types: (1) N-terminal kinesins, which move toward the plus end of microtubules and have a head motor domain located in the N-terminal, (2) M-kinesins, which specialize in depolymerization of microtubules and have the head motor domain situated in the middle of the amino acid sequence, and (3) C-terminal kinesins, which move toward the minus end of microtubules and have the head motor domain in the C-terminal (Hirokawa et al. 2009). Moreover, according to a variety of features, kinesins have so far been divided into 14 families (Miki et al. 2001; Lawrence et al. 2004). Members of kinesin superfamily proteins are continuously found in neuron cells (Hirokawa et al. 2009), somatic cells (Noda et al. 2001; Bernasconi et al. 2008), and testes (Sperry and Zhao 1996; Zou et al. 2002; Yang and Sperry 2003), which perform different functions.

In this large family, members of the C-terminal family move from the plus end to the minus end along microtubules, which is a significant departure from other members; we assume that they may have some specific functions during the transformation of spermatids. C-terminal kinesins are members of the kinesin-14 family, which consists of the kinesin-14A and -14B families (Miki et al. 2005). It is reported that members of this subfamily are required in multiple cellular processes including mitosis, cytokinesis, and organelle transportation (Miki et al. 2005; Walczak et al. 1997; Ems-McClung et al. 2004; Goshima and Vale 2005; Cai et al. 2009). So far, we have identified most of C-terminal members, including KIFC2, which mainly participates in the transportation of synaptic vesicles in dendrites (Saito et al. 1997), and KIFC3, which is mainly involved in intracellular transport of cilia and flagella (Noda et al. 2001; Xu et al. 2002). KIFC1 belongs to the kinesin-14 subfamily, a group of highly related C-terminal motor proteins with divergent tail domains (Hirokawa and Takemura 2004; Sperry and Zhao 1996; Zhang and Sperry 2004; Mountain et al. 1999).

Since KIFC1 was originally discovered in mouse embryonic brain (Saito et al. 1997), many homologs of KIFC1 have been identified in a diverse number of species and multiple physiological functions have been attributed to this protein. For example, *Drosophila melanogaster* NCD, a homolog of KIFC1, plays a crucial role in spindle pole formation in mitosis and meiosis (Endow et al. 1994), CTK2 (KIFC1 homologs in *Xenopus laevis*) is essential for mitotic spindle formation in egg extracts (Walczak et al. 1997; Zhang and Sperry 2004), and in mouse liver, KIFC1 is involved in motility and fission of early endocytic vesicles (Nath et al. 2007). Similarly, in rat liver, KIFC1 can mediate minus-end-directed motility of early endocytic vesicles integrated with Rab1a (Mukhopadhyay et al. 2011). Using siRNA interference to prevent KIFC1 expression, normal bipolar spindle formation is abrogated in cultured human cells (Zhu et al. 2005). Moreover, KIFC1 plays a pivotal role in acrosome formation, nuclear shaping, and flagellum formation during spermiogenesis. For instance, Yang and Sperry have reported that KIFC1 is first seen delivered with Golgi-originated vesicles and is then related to the growing acrosome of the spermatids during rat spermiogenesis. They are also associated with the reshaping and elongation of the spermatid nucleus through interaction with a nucleoporin (NUP62) and importin β. KIFC1 participates in the formation of acrosome, maintaining the configuration of the manchette which is close to the nuclear membrane (Yang and Sperry 2003; Yang et al. 2006). In crustaceans, such as *Macrobrachium nipponense* (Li et al. 2010; Wang et al. 2012) and *Exopalaemon modestus* (Hou and Yang 2013), KIFC1 is involved in acrosome formation and cell morphological changes by interacting with the AFS and LCx during spermiogenesis. And, KIFC1 is also responsible for vesicle transport from Golgi apparatus to growing acrosome and may be involved in perforatorium biogenesis of Chinese mitten crab (Yu et al. 2009). In cephalopods, including *Octopus tankahkeei* (Wang et al. 2010b, c) and *Sepiella maindroni* (Tan et al. 2013), KIFC1 is responsible for acrosome biogenesis through transport of the Golgi vesicle and nuclear reshaping. In amphibians, KIFC1 is also indispensable for the initiation of flagellum formation during spermiogenesis of *Eumeces chinensis* (Hu et al. 2013). However, unlike the above species, the sperm of teleost did not have an acrosome; to date, no studies have characterized the expression and function of the KIFC1 homolog in

the formation of acrosome-free sperm in teleost. Therefore, in order to explore this relationship between KIFC1 and spermiogenesis in teleost, we choose *Larimichthys crocea* as our experimental animal model.

L. crocea belongs to the Osteichthyes, Perciformes, and Sciaenidae classes of fish, which are mainly distributed in eastern coastal regions of Asia, and is one of the traditional economically important marine fish species in China. Spermatogenesis in teleost can be classified into four successive phases: spermatogonia, spermatocyte, spermatid, and spermatozoon phases. The mature sperm of *L. crocea* is composed of an oval or slightly elongated head and a flagellum; there is no acrosome in this species. KIFC1 contributes to nuclear deformation and flagella formation; however, its role in the spermiogenesis of *L. crocea* is not yet clear. Based on the review of abundant evidence, we hypothesized that the functions of KIFC1 are evolutionarily conserved during spermiogenesis, which means that *lc*-KIFC1 has a similar role as its homologs in other species. In this paper, we studied the characterization of *lc*-*kifc1* and the dynamic distribution of its mRNA and protein during spermiogenesis of *L. crocea*. We described the **a** cDNA sequence and protein structure analysis of *lc*-KIFC1, **b** protein sequence alignment and phylogenetic analysis of *lc*-KIFC1, **c** mRNA expression pattern in various tissues and different developmental stages of testis, and **d** spatial and temporal mRNA expression, and protein dynamic distribution of *lc*-KIFC1 during spermiogenesis.

Material and methods

Animal and sampling

All experiments were conducted in accordance with principles and procedures approved by the Animal Care and Use Committee of Ningbo University. Large yellow croaker used in this study was provided from cages in Xiangshan Harbor, Ningbo, China, from August 2015 to June 2016. In all, 20 male individuals with various maturities were selected according to the histological characteristics observed through paraffin section method. The animals were dissected immediately, and various tissues were extracted and preserved in different fixatives. For histological observations, some testes were fixed in the Bouin's solution for paraffin embedding and some were fixed in 2% glutaraldehyde for

electrical telescope observation. For cDNA cloning and qRT-PCR, different periods of testes and various tissues (testis, heart, liver, brain, gill, intestine, kidney, spleen, and muscle) were immediately frozen in the liquid nitrogen and then stored at −80 °C. Meanwhile, the testes from six different mature male animals were also subjected to fixation with 4% paraformaldehyde in phosphate-buffered saline (PBS; pH 7.4) for in situ hybridization and immunofluorescence.

Isolation of total RNA and synthesis of cDNA

Total RNA was extracted from various tissues and different developmental stages of testes by using TRIzol Reagent (Invitrogen, CA, USA) according to the methods in the manufacturer's manual. Firstly, we quickly grinded the dissociated tissue sample with liquid nitrogen and treated with TRIzol, chloroform, isopropanol, and then 75% ethanol sequentially to get precipitated RNA. Then, the precipitated RNA was re-suspended in 30 μL DEPC–H$_2$O, and the quality of extracted RNA was determined by spectrophotometer and agarose gel electrophoresis. Finally, the RNA sample was stored at −80 °C for reverse transcriptions.

The PrimeScript® RT reagent Kit (Takara, China) was used for ordinary reverse transcription assays. The Smart RACE cDNA Amplification Kit (Clontech, USA) was used for 5′ and 3′ RACE reverse transcription. For real-time quantitative PCR, first-strand cDNA was synthesized from 1000 ng total RNA by PrimeScript® RT reagent Kit with gDNA Eraser (Takara, China). The reverse transcription products were stored at −20 °C for future PCR.

Degenerate primer design and full-length cDNA cloning

Based on the highly conserved nucleotides of homologous sequence of *kifc1* genes in different species available from the National Center for Biotechnology Information (http://www.ncbi.nlm.nih.gov/, NCBI), we designed the first pairs of degenerate primers F1/R1 (Table 1) and other primers by Primer Premier 5.0 software in order to obtain the intermediate segment sequence of *kifc1*. For amplifying the fragment, the program was performed as follows: first, initial denaturation at 94 °C for 5 min, then 35 cycles (denaturation at 94 °C for 30 s, annealing at about 55 °C for 30 s, and extension at 72 °C for 30 s), finally extension at 72 °C for 10 min. However, the 3′ and 5′ end sequences of the

Table 1 The list of all primers used in this study

Primer name	Sequence (5′-3′)	Purpose
F1	GAGYGRCTGAAMTGGRGAGGG	Degenerate PCR
F2	TCMGAGTRTTYTGTAGVGTGCG	Degenerate PCR
R1	CGCAGDGTCTCRTTGTARAT	Degenerate PCR
R2	CACTVGCAGTHCCAATKACAC	Degenerate PCR
GSP-F1	GCTCCTCTCGCTCCCATTCAGTCTT	3′ RACE
GSP-F2	TGTCCAACCTGGGCATCGTCATC	3′ RACE
GSP-R1	CTGGGCTGTGGAGCGATTCTGATTGG	5′ RACE
GSP-R2	TCCATTTCAGTCACTCTCATCTTGCTC	5′ RACE
UPM-Long	CTAATACGACTCACTATAGGGC-	3′/5′ RACE
UPM-Long	-AAGCAGTGGTATCAACGCAGAGT	3′/5′ RACE
UPM-Short	CTAATACGACTCACTATAGGGC	3′/5′ RACE
NUP	AAGCAGTGGTATCAACGCAGAGT	3′/5′ RACE
RT-F	GCCAATCAGAATCGCTCCAC	Quantitative RT-PCR
RT-R	CTGATGACGATGCCCAGGTT	Quantitative RT-PCR
β-Actin F	TTATGAAGGCTATGCCCTGCC	Internal control of qRT-PCR
β-Actin R	TGAAGGAGTAGCCACGCTCTGT	Internal control of qRT-PCR
PROBE-F	AGAGCCCGTCAAACCACAC	In situ hybridization
PROBE-R	CCTCATACTCACTGATCTGGCTC	In situ hybridization

cDNA obtained from degenerate primer by PCR were incomplete. Therefore, together with generic primers UPM and NUP (Table 1), gene-specific primers (GSP) (Table 1) were designed for 3′ and 5′ rapid amplification of cDNA ends (RACE) which was performed by Nested PCR. According to the manufacturer's protocol, the first-round PCR was run as follows: 5 cycles of 94 °C for 30 s, 72 °C for 2 min; 5 cycles of 94 °C for 30 s, 70 °C for 30 s, and 72 °C for 2 min 30 s; 25 cycles of 94 °C for 30 s, 68 °C for 30 s, and 72 °C for 2 min 30 s, and a final extension of 72 °C for 8 min. After the first-round PCR, the amplified products were diluted 30 multiples to be used as the template of the second-round PCR, which was run as follows: 94 °C for 4 min, 35 cycles of 94 °C for 30 s, 68 °C for 30 s, and 72 °C for 2 min, and a final extension of 72 °C for 8 min. Subsequently, the PCR products were separated by agarose electrophoresis and the bands visualized by Gelview. The expected bands were extracted and purified using Quick-type DNA Gel Extraction Kit (Bioteke, Beijing, China). The purified fragments were ligated into the PMD-18T vector (Takara, Dalian, China) and then transformed into competent cells (Escherichia coli DH5α), and finally sequenced by Beijing Genomics Institute (Beijing, China). In the end, the full-length cDNA was established by combining the 5′ RACE fragment, the originally derived fragment, and the 3′ RACE fragment.

Sequence characterization and phylogenetic analysis

The sequences of lc-kifc1cDNA and protein were analyzed for similarity with known sequences in the nonredundant GenBank database using BLAST online provided by NCBI. For the conservation analysis of KIFC1 proteins, the multiple sequence alignment of homogenous proteins from different species was produced by Vector NTI10 software and the phylogenetic tree was constructed with the neighbor-joining method of MEGA version 5.0 software. In the meantime, the putative secondary and tertiary structures of KIFC1 proteins were predicted using UniProt (http://www.uniprot.org/) and I-TASSER (http://zhanglab.ccmb.med.umich.edu/I-TASSER/), respectively. We used the KIFC1 homologs in different species for comparison and their GenBank accession numbers were as follows: Mus musculus (AAI00329.1), Rattus norvegicus (AAH83827), Homo sapiens (AAI21043.1), Gallus gallus (BAF62975.1), Xenopus laevis (NP_001081003.1), Salmo salar (ABQ59663.1), Danio rerio (CAD60638.1), Eumeces chinensis (JF274260), Eriocheir sinensis (GU990077), Macrobrachium rosenbergii (JN627516), and Octopus tankahkeei (GU980701).

Quantitative real-time PCR analysis of kifc1 mRNA expression in different tissues and testes at different developmental stages

Nine different tissues collected from six individuals of male fishes and different periods of testes selected from approximate 20 male fishes at four successive developmental stages were used to extract total RNA for qRT-PCR, aiming at knowing about the expression levels and patterns of kifc1 mRNA. Specific primers of lc-kifc1 and lc-β-actin for qRT-PCR were designed by Primer Premier 5.0 software (Table 1) and were tested after PCR to ensure no other product except the expected on the basis of analyses of the melting curve and electrophoretogram. Reactions were performed with SYBR® Premix Ex TaqTM II (Takara, China) and analyzed in the ABI Prism 7900HT Sequence Detector System. The qRT-PCR amplifications were run according to the following cycling conditions: 95 °C for 5 min activation, followed by 40 cycles of 95 °C for 20 s, 60 °C for 20 s, and 72 °C for 20 s, and a final extension of 72 °C for 10 min. The final step was to obtain a melt curve for the PCR products to determine the specificity of amplification. All samples were examined in triplicate on the sane plate ($n = 3$). Eventually, the expression levels of kifc1 mRNA were calculated by means of the $2^{-\Delta\Delta Ct}$ method. All quantitative data were presented as the means ± standard deviation (SD). The statistical analyses were carried out with SPSS 17.0 (USA), and statistical significant difference of expressions was defined as $p < 0.05$.

Light microscopy (LM)

For light microscopy, excised testis tissues were fixed in Bouin's solution for about 24 h, the specimens providing the testes were dehydrated in a graded ethanol series (70, 80, 90, 95, and 100%) and later immersed transparent tissues in paraffin. Serial sections were cut at a thickness of about 7 μm. The histological sections were stained with hematoxylin-eosin (HE) then examined using an Olympus BX51 light microscope and photographed with Image-Pro Plus 6.0 software for observing the morphological characteristics of the cells.

Transmission electron microscopy

For transmission electron microscopy, the testes were cut into small pieces and fixed in 3% glutaraldehyde buffer at 4 °C for 2–4 h and testis specimens were rinsed in 0.1 M phosphate buffer (pH 7.4) for several times. Thereafter, the samples were post-fixed in 0.1 M osmium tetroxide for 1–2 h in the dark. Following several short washings in 0.1 M phosphate buffer (pH 7.4), samples were dehydrated in a graded ethanol series (30, 50, 70, and 90%) and subsequently transferred to ascending concentrations of acetone (90 and 100%). Finally, samples were embedded in epoxy resin (Epon 812) and acetone (1:1) for 1 h, followed by araldite resin and acetone (2:1) for 1–1.5 h, and lastly in pure araldite resin for 1 h. Ultrathin sections were cut with a LKB-α ultramicrotome, stained with uranyl acetate for 40 min, and counterstained with lead citrate for 1 min for later examination using a JEM-1200EX transmission electron microscope.

In situ hybridization

Tissue preparation

Testes from male *L. crocea* were quickly dissected and then embedded into an optimum cutting temperature (O.C.T) compound, which was snap frozen with liquid nitrogen and later stored at −80 °C. These blocks were cut into 6-μm sections at −20 °C using a freezing microtome. Finally, the tissue sections were mounted onto the RNase-free poly-l-lysine-coated slides that were rapidly transferred to −80 °C.

Riboprobe synthesis

The two special primers (Table 1) were used to amplify the target cDNA fragment (425 bp) for riboprobe synthesis. The PCR was run as follows: 94 °C for 5 min; 35 cycles of 94 °C for 30 s, 57 °C for 30 s, and 72 °C for 30 s; and 72 °C for 10 min for the final extension. The target cDNA products were sequentially inserted into the PGEM-T EASY Vector (Promega, USA), transformed into DH5α, and sequenced by Beijing Genomics Institute (Beijing, China). The cDNA-containing plasmids were extracted using AxyPrep Plasmid Miniprep Kit (Axygen) and linearized with QuickCut SpeI (Takara) at 37 °C for 5 min. Then, the product was purified and utilized as the template for riboprobe

synthesis by transcribing with T7 RNA polymerase (Promega, USA) and DIG-UTP (Roche, Germany) in RNase-free environment. Riboprobes were precipitated by pre-chilled ethanol and LiCl for 1 h at −80 °C, resuspended in DEPC-treated H$_2$O. Finally, riboprobes concentration and quality were detected by spectrophotometer and nucleic acid electrophoresis, respectively.

Pre-hybridization and hybridization

The tissue sections were placed at room temperature for 10 min and then fixed with 4% paraformaldehyde (PFA, pH 7.4) for 10 min. Later, the slices were rinsed for 10 min in 0.1% diethylpyrocarbonate (DEPC)-activated 0.1 M phosphate-buffered saline (PBS, pH 7.4) at room temperature twice and equilibrated for 15 min in 5 × SSC (sodium chloride 0.75 M, sodium citrate 0.075 M, pH 7.0). Afterward, the sections were initially placed into pre-hybridization buffer containing 50% deionized formamide, 40 μg/mL denatured salmon sperm DNA, and 5 × SSC solution for 2 h at 55 °C. The probe denaturation was conducted for 5 min at 80 °C and then frozen for 2 min, and the hybridization was performed in hybridization mixture with approximately 400 ng/mL of DIG-labeled riboprobe in the same wet box saturated with 5 × SSC solution that contained 50% formamide at 55 °C overnight. Following this reaction, the sections were sequentially rinsed for 30 min in 2 × SSC (pH 7.0) at room temperature; 1 h in 2 × SSC (pH 7.0) at 65 °C water bath; and 1 h in 0.1 × SSC (pH 7.0) at 65 °C water bath.

Detection of hybridization product

The sections were equilibrated for 5 min in Buffer I (0.1 M Tris-HCl and 0.15 M NaCl, pH 7.5) and then incubated for 2 h at room temperature with anti-DIG alkaline phosphatase-conjugated Fab fragments (Roche) diluted 1:2000 in Buffer I containing 0.1% blocking reagent (Roche). The sections were washed three times and each time for 15 min in buffer I and then balanced with buffer II (0.1 M Tris-HCl, 0.1 M NaCl, and 0.05 M magnesium chloride, pH 9.5) at room temperature for 5 min. Then, the chromogenic reaction was performed in buffer II containing 330 μg/mL nitroblue tetrazolium chloride (NBT) (Promega) and 165 μg/mL, 5-bromo-4-chloro-3-indolylphosphate (BCIP) (Promega) in darkness for 2 h at room temperature. The reaction was terminated by washing in TE buffer (10 mM Tris-HCl,

1 mM EDTA, pH 8.0) for 10 min. Non-specific staining was removed by immersion in 95% ethanol with a gentle rinse for 1.5 h. After all these steps, the sections were rehydrated for 15 min in deionized water to remove precipitated Tris, dehydrated through successive baths of ethanol (50, 70, 95, and 100%) and xylol (15 min each) for two times, and mounted with gelatin. The hybridized sections were observed and photographed under an Olympus BX51 inflorescence microscope (Olympus) under bright-field illumination.

Western blot

Testes from mature large yellow croaker were homogenized in RIPA Lysis Buffer (Beyotime, Shanghai, China) containing protease inhibitors. The homogenates were centrifuged at 14,000 rpm at 4 °C for 15 min and the supernatant liquids were collected. The protein concentrations were detected by the Coomassie brilliant blue method, and the protein samples were dissolved in 5 × SDS sample buffer. The protein samples with equal amounts of protein were separated on 8% gels (SDS-PAGE) and transferred onto the PVDF membrane (Bio-Rad, California, USA). The membrane was blocked with 5% BSA in PBST (PBS with 0.5% Tween 20) for 1 h and then the membrane was incubated overnight at 4 °C with rabbit anti-KIFC1 antibody (diluted 1:400) in 5% BSA. After washing three times with PBST for 1 h, the membrane was incubated for 1 h with secondary antibody HRP-conjugated goat anti-rabbit IgG (diluted 1:1000) in 5% BSA. After that, the membrane was washed three times with PBST for 45 min, three times with PBS for 30 min and three times with ultrapure water for 15 min. The emitted light was detected using a chemiluminescence imaging (Tanon 5200) (Shanghai, China).

Immunofluorescence

Testes were dissected from various maturities large yellow croaker and fixed in 4% paraformaldehyde (PFA, pH 7.4) overnight at 4 °C, washed in PBS three times for 15 min. Then, they were incubated in 0.5 M sucrose-PBS (pH 7.4) at 4 °C until they sunk, followed by embedding in OCT compound at −20 °C. The tissues were cut into 6 μm frozen sections and transferred to slides. After drying at 37 °C, the sections were treated with PBST (PBS with 0.3% Triton X-100) for 15 min at room temperature and then blocked with 5% BSA in PBST (0.1% Triton X-100) for 1 h. The tissue sections were incubated with rabbit anti-KIFC1 antibody (diluted 1:100) in blocking buffer 3% BSA at 4 °C overnight. The sections were rinsed three times in 0.1% PBST for 15 min. The tissue sections were then incubated with Alexa Fluor 488-labeled Goat Anti-Rabbit IgG (H + L) (Beyotime) and Tubulin-Trakcer Red (Beyotime) secondary antibodies for 1 h at room temperature. The sections were rinsed six times in 0.1% PBST (each for 15 min). The nuclei were stained with DAPI (Beyotime) for 5 min. The immunostained tissue sections were mounted in Antifade Polyvinylpyrrolidone Mounting Medium (Beyotime). The immunostained tissue sections were observed with a Confocal Laser-scanning Microscope (LSM880) (Carl Zeiss, Germany).

Results

Full length of *lc-kifc1* cDNA sequence

The coding region of *lc-kifc1* was cloned using degenerated PCR, and the untranslated regions (UTRs) were acquired by RACE. The complete *lc-kifc1* sequence (GeneBank accession number KU198279) was 2481 bp in length containing a 53 bp 5′ UTR, a 535 bp 3′ UTR and a 1893 bp open reading frame (ORF) that encoded the *lc*-KIFC1 protein of 630 amino acids (Fig. 1). The calculated molecular weight of the putative *lc*-KIFC1 was 69.3 kDa, and the estimated isoelectric point (PI) was 9.20 (http://web.expasy.org/protparam/).

Putative structure of *lc*-KIFC1 protein

Secondary structural analysis was conducted for the putative *lc*-KIFC1. The analysis showed that *lc*-KIFC1 had three domains: a C-terminus, stalk region, and N-terminus. Amino acids 287–630 constitute the putative C-terminus and contain the conserved motor domain that may form a globular head for movement along the microtubules. Amino acids 124–287 constitute the stalk region that forms an extended coiled-coil stalk with changing direction. Amino acids 1–124 constitute the N-terminus with a divergent tail to transport different cargos (Fig. 2a). Tertiary structure prediction showed an interesting structure resembling a sideways "Y" shape (Fig. 2b). The N-terminal divergent tail domain particularly binds the specific cargo. The C-terminal head domain has microtubule and ATP binding sites, which

```
                                                              M   S   R   L   P   V   M   T   S   K   R   V   L
   1 GGCAGACGGAGCCGGAGGAGTCCCGGCGGAGAACCAGCGGCGCTAAAGAGACCATGTCCCGCTTACCAGTCATGACAAGCAAACGGGTCC
  14  T   S   S   S   S   E   N   S   Q   D   M   A   P   A   Q   K   K   L   R   K   D   P   E   P   V   K   P   H   A
  91 TTACAAGCAGCAGCAGCTCTGAGAACAGCCAAGACATGGCACCCGCTCAGAAGAAGCTTCGTAAGGACCCAGAGCCCGTCAAACCACACG
  44  A   A   T   I   I   G   G   K   R   P   P   V   A   A   T   R   A   P   I   S   R   S   V   R   A   V   G   A   A   T
 181 CAGCAGCTACAATCATCGGTGGCAAGCGTCCTCCTGTTGCTGCGACCAGAGCACCCATCTCTAGGTCAGTCAGAGCTGTGGGAGCTGCCA
  74  V   A   V   G   P   S   R   G   V   L   K   P   S   V   A   S   A   A   P   K   G   G   N   M   K   Q   T   A   A   P
 271 CTGTGGCTGTTGGTCCTTCCAGAGGTGTCCTGAAACCATCTGTAGCTTCAGCTGCACCAAAGGGAGGCAACATGAAACAAACTGCGGCAC
 104  T   G   T   K   P   G   G   G   G   T   K   R   H   A   W   D   L   K   G   K   V   S   D   M   E   G   K   L   R   N
 361 CCACTGGTACAAAACCAGGTGGTGGTGGTACCAAGCGGCATGCATGGGACCTGAAGGGCAAGGTCAGCGACATGGAGGGAAAGCTCCGTA
 134  Y   Q   S   K   V   K   S   V   N   E   E   N   D   I   L   K   G   T   M   V   Q   S   K   M   R   V   T   E   M   E
 451 ACTACCAGTCCAAGGTGAAATCTGTCAACGAGGAGAATGACATTCTTAAAGGCACGATGGTCCAGAGCAAGATGAGAGTGACTGAAATGG
 164  R   E   L   K   R   Q   Q   S   Q   I   S   E   Y   E   D   E   L   H   A   L   S   G   V   R   D   K   L   E   K   V
 541 AGAGGGAGCTGAAGAGGCAGCAGAGCCAGATCAGTGAGTATGAGGACGAGTTACATGCGTTGTCAGGAGTCCGGGACAAGCTGGAGAAAG
 194  S   S   D   K   S   T   L   Q   K   E   L   S   N   L   E   G   K   Y   K   V   M   E   T   L   R   D   S   Q   E   T
 631 TCTCCAGTGATAAAAGTACTCTTCAGAAGGAGCTCTCCAACTTGGAGGGCAAGTACAAAGTCATGGAGACTCTCCGAGACAGTCAGGAGA
 224  E   L   Q   T   L   T   V   K   L   S   V   L   E   S   T   L   A   R   L   Q   G   T   L   R   D   T   E   E   E   V
 721 CAGAGCTGCAAACTCTCACGGTGAAGCTTTCAGTGCTGGAGTCGACTCTAGCCCGCCTGCAGGGGACCCTCAGAGACACAGAGGAAGAGG
 254  R   S   L   K   E   T   V   A   E   Q   K   D   E   L   H   A   G   E   M   E   R   R   R   L   H   N   T   I   Q   E
 811 TGCGCTCTCTCAAAGAGACCGTGGCTGAGCAGAAAGACGAGCTTCATGCTGGGGAGATGGAGCGCAGGCGGCTTCACAATACCATCCAGG
 284  L   K   G   N   I   R   V   F   C   R   V   R   P   L   V   D   G   G   L   S   K   H   I   Q   L   P   T   S   D   I
 901 AGCTCAAGGGCAATATCAGAGTGTTCTGTAGAGTGCGCCCACTGGTGGACGGAGGCCTCAGCAAACACATTCAGCTCCCGACTAGTGACA
 314  K   T   I   T   L   A   K   T   E   E   S   H   T   G   K   T   A   D   T   Q   K   N   Y   N   F   N   F   D   R   V
 991 TCAAGACCATAACGCTGGCCAAAACAGAGGAGTCTCACACAGGCAAAACTGCAGACACTCAGAAGAATTACAACTTCAACTTTGATCGCG
 344  F   G   P   G   A   S   Q   Q   E   V   F   E   E   I   S   L   L   V   Q   S   A   L   D   G   Y   N   V   C   C   F
1081 TATTTGGCCCCGGGGCTTCACAGCAGGAGGTCTTTGAAGAGATCTCTCTGCTGGTGCAGTCAGCACTGGACGGCTACAACGTCTGCTGCT
374  A   Y   G   Q   T   G   S   G   K   T   Y   T   M   E   G   D   E   F   D   K   T   R   G   V   I   P   R   A   V   Q
1171 TTGCCTATGGCCAGACAGGGAGTGGAAAGACGTACACCATGGAGGGAGACGAGTTTGATAAGACCAGAGGTGTCATTCCCAGAGCCGTGC
404  Q   I   F   R   A   A   E   K   L   A   T   Q   G   W   E   F   T   F   T   A   S   F   V   E   I   Y   N   E   T   L
1261 AGCAAATCTTCAGAGCAGCAGAGAAGCTGGCAACACAGGGCTGGGAGTTCACCTTCACGGCGAGCTTTGTTGAAATTTACAACGAGACCC
434  R   D   L   L   Y   T   G   K   A   S   K   R   P   E   H   E   I   R   K   S   T   N   N   E   V   T   I   T   N   L
1351 TGCGGGACCTCCTCTACACTGGGAAGGCCAGCAAGAGGCCCGAGCATGAGATCCGGAAGTCGACCAACAATGAGGTGACCATCACCAACC
464  T   Y   E   K   V   S   N   E   D   Q   V   L   G   L   I   A   L   A   N   Q   N   R   S   T   A   Q   T   A   Q   N
1441 TCACCTACGAGAAGGTCTCCAACGAGGATCAGGTCCTCGGCCTCATCGCTTTGGCCAATCAGAATCGCTCCACAGCCCAGACGGCCCAGA
494  D   R   S   S   R   S   H   S   V   F   Q   L   D   I   E   G   V   N   A   G   R   D   V   K   C   K   S   T   L   C
1531 ACGACCGCTCCTCTCGCTCCCATTCAGTCTTCCAGCTGGATATCGAGGGAGTGAATGCTGGCAGGGATGTCAAATGCAAGTCCACTCTGT
524  L   V   D   L   A   G   S   E   R   M   L   K   S   Q   S   Q   G   E   R   F   K   E   M   T   A   I   N   G   S   L
1621 GCCTGGTGGACTTGGCTGGCAGCGAGCGAATGCTGAAGAGTCAGTCTCAGGGTGAACGCTTCAAAGAGATGACGGCCATCAACGGCTCCC
554  S   N   L   G   I   V   I   S   A   L   A   N   K   E   S   Y   V   P   Y   R   N   S   K   L   T   Y   L   L   Q   G
1711 TGTCCAACCTGGGCATCGTCATCAGCGCGCTGGCCAACAAGGAGAGCTACGTTCCGTACAGGAACTCCAAGCTTACCTACCTTCTGCAGG
584  C   L   G   G   N   S   K   T   L   M   F   V   N   I   A   P   E   S   D   S   F   G   E   T   L   N   S   L   R   F
1801 GCTGCTTGGGAGGAAACAGCAAAACCCTGATGTTTGTGAACATCGCCCCGGAGTCAGACAGTTTTGGGGAAACCCTCAACTCCTTGAGGT
614  A   S   K   V   N   D   C   V   I   G   T   A   S   A   N   R   K   *
1891 TCGCCAGCAAGGTGAACGACTGTGTAATTGGGACTGCGAGTGCCAACAGGAAGTAGTGCGGCGTGCTTAAAAGAAACTCTATTCTTACCT
1981 TTTTTATTATTATTATTATTACGGTCACAACATGAAATGTTCAGTGTAATTGTTTCCAGTAGCTTGTACTTTCACATTGTGCTGTTTGAC
2071 ACACGCTTTGGTGCCAACCAGTAAAAACCAAAACATCTGTTTGTATATTTTCAGGACTTTGATCACTAATACAAGCTTTTAAACATTTTT
2161 ATGCCTCTGTGTAAATCAAGTGTATGTGTACATACGCGTTATTCTATCCAGATTTTTCTTTCTTTTTAAATGCATGATCGGCCTCTTGAC
2251 TTATGATTTAACAGACATTTAATCTCTCTTTTCATTTACGCATGTTTAAGTGTGTTACATATACTTGTAGTGCAATTAAACTCATACTGT
2341 CATTTTTGTTTAGTTTTTTCTTTGGATCTGTGTTCGAAGGTGTGTTTGTTTTTGTGCTCACCTCTGGCCCAACATAATAAAGACATTCAG
2431 TGGCTGAGCTACTGACTGCTAAAAAAAAAAAAAAAAAAAAAAAAAAAAAAAAAAA
```

provide dynamic energy. Between these parts, the stalk domain serves as a link to stabilize the conformation of the protein and ensure the precise orientation of the transportation.

Protein sequence alignment and phylogenetic analysis

The predicted *lc*-KIFC1 protein was aligned with its homologs in different species (Fig. 3). The results showed that the amino acid sequence of *lc*-KIFC1 shared 73.2, 49.8, 49.3, 54.6, 56.5, 53.1, and 52.1% identity with its counterparts in *Danio rerio*, *Eriocheir sinensis*, *Octopus tankahkeei*, *Gallus gallus*, *Xenopus laevis*, *Mus musculus*, and *Homo sapiens*, respectively. We assumed that the KIFC1 protein is evolutionarily conserved. KIFC1 in *L. crocea* has high homology with KIFC1 in *D. rerio*. The alignment results indicate that the deduced KIFC1 protein possesses three ATP-binding sites (AYGXTGXGKX,

SSRSH, and LAGSE) and one microtubule-binding site (YXXXXXDLL) in its motor domain at the C-terminal region (Miki et al. 2001; Ho et al. 2008). In addition, *lc*-KIFC1 also contained the KIFC conserved consensus ELKGN sequence (Saito et al. 1997) and the β1 strand RVFCRVRP domain which connect the stalk and motor domain, and may change its conformation to adjust the direction of movement of the stalk and loading of cargo to the tail (Saito et al. 1997). From phylogenic analysis, we corroborated that the results from the multiple sequence alignment that the putative protein *lc*-KIFC1 was closest to that of *D. rerio* among the other examined species (Fig. 4).

Tissue distribution of *lc-kifc1* mRNA

The expression of *lc-kifc1* mRNA in different tissues of the *L. crocea* was measured by qRT-PCR using β-actin as an internal control. We amplified a 241 bp *lc-kifc1* cDNA fragment from the testis, heart, liver, brain, gill, intestine, kidney, spleen, and muscle of *L. crocea*. Results showed that expression of *lc-kifc1* mRNA occurs in all of the above-mentioned tissues with an abundance of expression in the testis; expression is relatively weak in the heart, liver, and kidney. In addition, *lc-kifc1* has little to no expression in other remaining tissues (Fig. 5a).

A

NH₂ | Tail | Stalk | Head | COOH

1   124   287   630

B
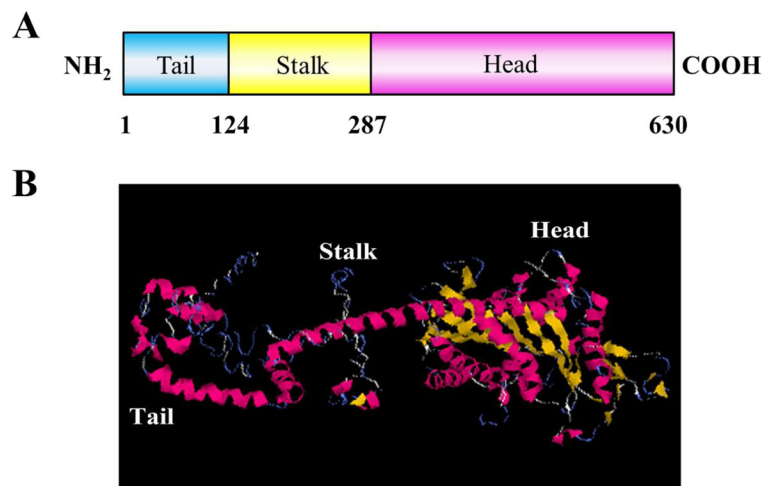
Fig. 2 The major structural features of *L. crocea* KIFC1. **a** This figure shows the three structural domains of KIFC1. The C-terminus (287–630 aa) contains the conserved motor domain (*pink bar*) that may form a globular head for moving along microtubules. The central region (124–287 aa) forms an extended coiled-coil stalk with changing direction (*yellow bar*). The N-terminus (1–124 aa) contains the divergent tail (*blue bar*) that transports different cargos. **b** This figure shows the putative 3-D structure of KIFC1. The protein structure of *lc*-KIFC1 is constituted by α-helix (*rose*), β-sheet (*yellow*), and strand (*blue*). The globular head consists of α-helix and β-pleated sheet, the stalk is mainly made up of α-helix, and the tail is mainly made up of α-helix and strand
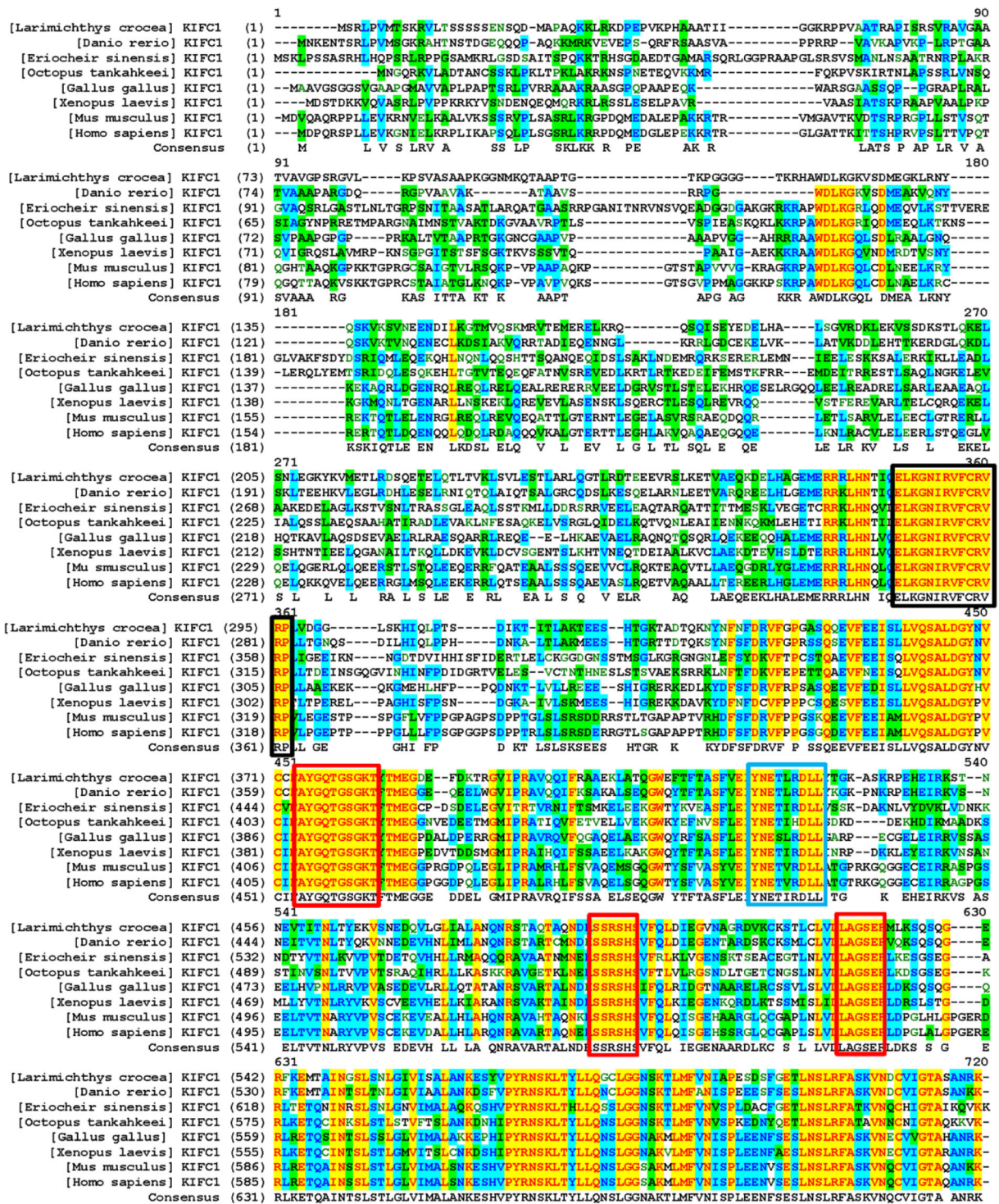
Fig. 3 Multiple sequence alignment of KIFC1 in *Larimichthys crocea* with its homologs, including *Danio rerio*, *Eriocheir sinensis*, *Octopus tankahkeei*, *Gallus gallus*, *Xenopus laevis*, *Mus musculus*, and *Homo sapiens*. The amino acid alignment was performed using Vector NTI10 (Invitrogen). The putative ATP-binding motifs contain the AYGQTGSGKT, SSRSH, and LAGSE sequences (*labeled red frame*) and the microtubule-binding motif, YNETLRDLL sequence was labeled by a *blue rectangle*. The KIFC1 conserved consensus ELKGN sequence was labeled by a *black rectangle* and the RVFCRVRP domain might represent the β1 strand (labeled by a *black rectangle*)
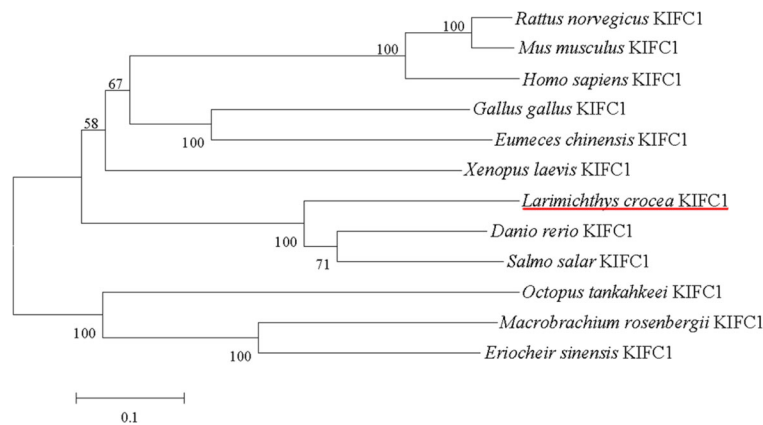
Fig. 4 Phylogenetic tree of KIFC1 homologs from various species was generated based on the alignment of amino acid sequences using MEGA 5.0 software using the neighbor-joining method. The *numbers* at nodes indicate the bootstrap values with a number of resampling of 1000. The KIFC1 homologs are as follows: *Mus musculus*, *Rattus norvegicus*, *Homo sapiens*, *Gallus gallus*, *Xenopus laevis*, *Salmo salar*, *Danio rerio*, *Eumeces chinensis*, *Eriocheir sinensis*, *Macrobrachium rosenbergii*, and *Octopus tankahkeei*. The putative *L. crocea* KIFC1 protein is most closely related to *Danio rerio*

Maturational changes in testis *lc-kifc1* mRNA expression

We also analyzed the expression of *lc-kifc1* mRNA in the testis over the four different growth stages during the same breeding season. Real-time PCR results indicated that during testis development, *lc-kifc1* mRNA expression had a tendency to steadily increase as development progressed, before decreasing greatly at the end of the development cycle. The lowest level of *lc-kifc1* mRNA expression was observed in stage II testes. In accordance with the progress of testis growth, *lc-kifc1* mRNA expression gradually and significantly increased in the testes during stages III–IV of development and reached a peak at stage IV. However, following stage V of development, *lc-kifc1* expression was sharply decreased but still higher than that of stage II testis (Fig. 5b).

Spatial and temporal mRNA expression of *lc-kifc1* during spermiogenesis

Using paraffin section and transmission electron microscopy (TEM), we obtained histological and ultrastructural information of the process of spermiogenesis in *L. crocea*. In combination with the results of in situ hybridization, the spatial-temporal expression pattern of *lc-kifc1* mRNA was determined. The main results of *lc-kifc1* mRNA expression indicated two parts: Firstly, in the process of spermiogenesis, *lc-kifc1* mRNA was expressed in most abundance around the nucleus and tail during the transformation from early spermatid to mature sperm; secondly, *lc-kifc1* mRNA probably participates in the reshaping of nucleus and formation of sperm tail.

As the results showed, in the early stage of spermatid, the shape of the cell was nearly round with various sizes of mitochondria in the cytoplasm, the nucleus was round or oval, there was nuclear chromatin condensation, and the flagellum began to appear. During this period, the expression of *lc-kifc1* mRNA was weakly distributed in the periphery of the nuclear membrane (Fig. 6a1, arrows; blue signal). In the middle stage of spermatid, cells were round or oval, the volume decreased slightly, and the nucleus was round; with nuclear chromatin condensation and gathered to the side of the clumps, the mitochondria had shifted to one end of the cell. During this stage, the signals for expressed *lc-kifc1* mRNA increased gradually and were mainly localized to the periphery of the nuclear membrane and side of the nucleus (Fig. 6a2, arrows; blue signal). In the late stage of spermatid, cells were irregularly shaped, the cytoplasmic volume was significantly reduced, the nucleus was diversiform, and chromatin condensation was further deepened. Multiple mitochondria surround the bottom of the nucleus and formed a midpiece structure. At this time, the flagellum gradually extended. In this period, the *lc-kifc1* mRNA signal was abundant and reached a peak, being mainly concentrated at one end of the nucleus, which suggests that *lc-kifc1* mRNA is involved in the condensation of nucleus and formation of flagellum (Fig. 6a3, arrows; blue signal). In the mature sperm, cells were spherical, the volume was significantly

Fig. 5 Quantitative RT-PCR analysis of *kifc1* gene expression in *Larimichthys crocea*. **a** This figure shows the *kifc1* expression in various tissues. Samples include the following: *B* brain, *G* gill, *H* heart, *M* muscle, *I* intestine, *L* liver, *T* testis, *S* spleen, *K* kidney. Liver served as control. **b** This figure shows the expression level of *kifc1* at different stages of testis development. Maturing testes were divided into four stages based on histological observations. The testis at stage II served as control. *Columns* indicate mean *kifc1* levels (relative to the inter-assay standard sample) and *error bars* indicate standard errors (*n* = 3). Mean values bearing *different letter superscripts* are significantly different (*p* < 0.05). β-Actin was used as a reference gene
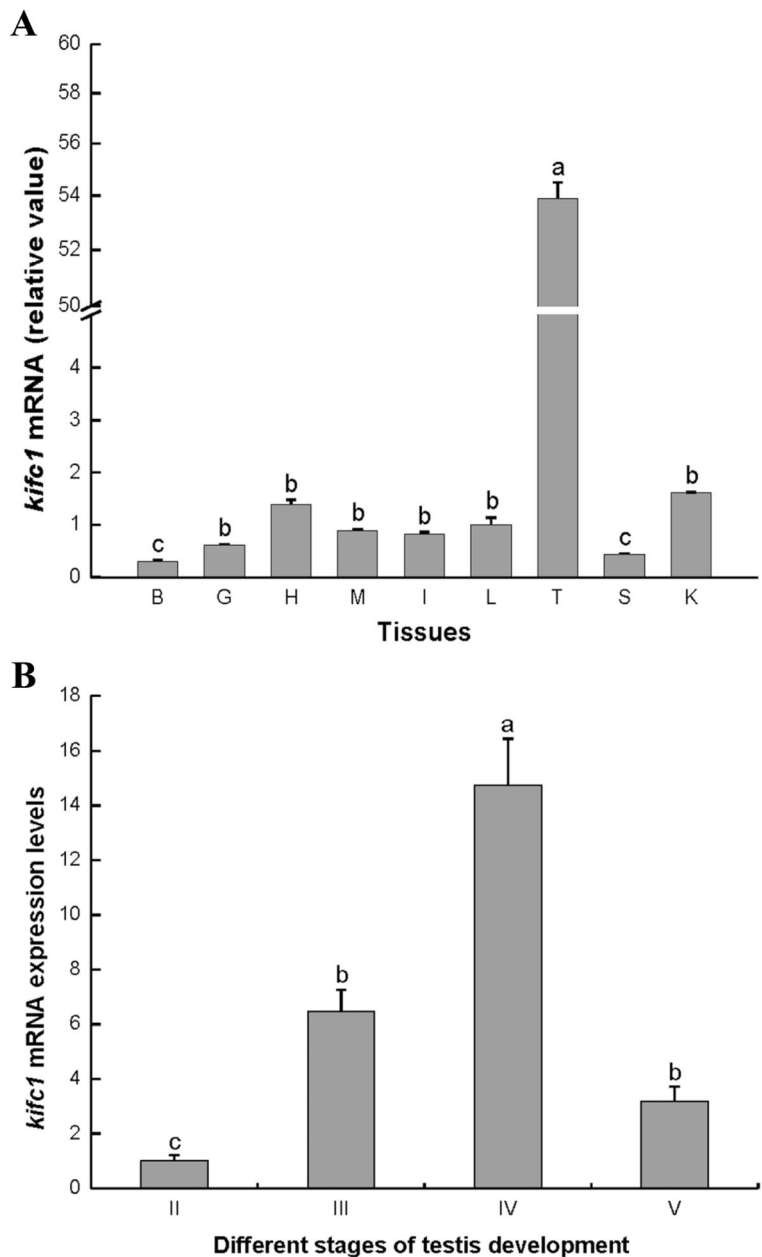
reduced, the nucleus accounting for a larger part than the cytoplasm, and the chromatin was highly concentrated in the nucleus. In the meantime, the mRNA signal of *lc-kifc1* was drastically weakened and only few signals still appeared in the tail (Fig. 6a4, arrows; blue signal). Negative controls including an antisense probe or no primary antibody showed no obvious hybridization signal (data not shown). In addition, the paraffin section and TEM results from the different stages of spermiogenesis in *L. crocea* are shown on Fig. 6b, c. A series of

schematic diagrams illustrating the spatial and temporal *lc-kifc1* mRNA expression patterns during spermiogenesis are shown in Fig. 6d.

Dynamic distribution of *lc*-KIFC1 protein during spermiogenesis

The specific of rabbit anti-KIFC1 antibody was detected by western blotting. The anti-KIFC1 polyclonal antibody recognized a probable 69 kDa band indicative of

KIFC1 (Fig. 7). Subsequently, in order to explore the relationship of KIFC1 and microtubules in cellular transformations during spermiogenesis, we analyzed the localization of KIFC1 and tubulin by immunofluorescence and laser scanning confocal microscopy. The results revealed that *lc*-KIFC1 and tubulin were co-localized around the nucleus during spermiogenesis. In the early stage of spermiogenesis, tubulin (Fig. 8a2, arrows; red signal) and *lc*-KIFC1 (Fig. 8a3, arrows; green signal) were weakly expressed in the cytoplasm and localized near the nuclear membrane. In the middle stage of spermiogenesis, the nucleus began to undergo complex morphological changes, with tubulin (Fig. 8b2, arrows; red signal) and *lc*-KIFC1 (Fig. 8b3, arrows; green signal) being highly expressed in the cytoplasm and the side of the nucleus. In the late stage of spermiogenesis when the midpiece began to form and flagellum gradually lengthen, *lc*-KIFC1 expression increased greatly and strong signals of *lc*-KIFC1 were mainly present at the one end of the nucleus (Fig. 8c3, arrows; green signal). Meanwhile, tubulin was still localized around the nucleus (Fig. 8c2, arrows; red signal). In the mature sperm, tubulin was distributed in the cytoplasm and one end of the nucleus (Fig. 8d2, arrows; red signal). However, the signal intensity of *lc*-KIFC1 was greatly decreased and was located in the midpiece and flagellum of the tail (Fig. 8d3, arrows; green signal). Finally, we also used immunofluorescent localization of MitoTracker (a mitochondria marker) in order to identify KIFC1 transport substrates involved in the formation of flagellum midpiece (Fig. 9). In the figure, red represents the KIFC1 protein signal and green represented the mitochondrial signal. As the results noticed, *lc*-KIFC1 signals co-localized with mitochondria at each stage during spermiogenesis. Additionally, mitochondria were localized in the same fashion as tubulin during the different stages of spermiogenesis in *L. crocea* (Fig. 9). Negative controls no primary antibody showed no obvious fluorescence signal (data not shown).

Discussion

Analysis of KIFC1's structure and conservation

KIFC1 is a member of the highly relevant group of C-terminal motor proteins that have extremely similar motor domains and diverse tail domains (Noda et al. 1995). The identification of the *lc-kifc1* gene indicates a function for KIFC1 in teleost and prompts further exploration of the function of the putative KIFC1 protein to establish a stable foundation. The full-length cDNA of *lc-kifc1* is 2481 bp in length, including a 53 bp 5′ UTR, a 1893 bp ORF encoding a protein with 630 amino acids, and a 535 bp 3′ UTR. Sequence analysis of the deduced protein shows a considerable homology with a group of KIFC1 homologs from diverse species. Multiple sequence alignment indicates that the carboxyl terminus of the putative protein is relatively conserved, but its amino terminus is significantly dissimilar among different homologs. The motor domain is located at the C-terminus which is the microtubule binding domain formed by the head that walks along the microtubules, and the function of stalk domain is to form an extended coiled-coil stalk, while the N-terminus possesses the cargo-binding property (Vale 2003). Thus, in this way, a similar force-generating mechanism provided by the motor domain is achieved, while the obvious cargo-binding domain confers assorted functions to individual KIFC1 homologs on specific occasions (Zhang and Sperry 2004; Cai et al. 2009). The comparison of the similarity with different species and the phylogenetic tree reveals that *lc*-KIFC1 holds the relative conservative which may be important for the functions of KIFC1 during the evolution.

Dynamic expression of the *lc-kifc1* gene in different tissues and testis developmental stages

Tissue expression pattern analysis of *lc-kifc1* mRNA by qRT-PCR indicated that its expression is high in the testes. This result may indicate an indispensable function of KIFC1 during spermiogenesis in *L. crocea*. In addition, *lc-kifc1* mRNA was also present in other examined tissues included that of the heart, liver, and kidney, which may suggest that KIFC1 has other important functions in these tissues. Previous research has demonstrated that KIFC1 was fairly abundant, widely distributed, and expressed in the mouse testis, ovary, spleen, and liver (Noda et al. 1995; Navolanic and Sperry 2000; Yang and Sperry 2003; Lawrence et al. 2004; Nath et al. 2007). In the mouse liver, KIFC1 was required for motility and fission of early endocytic vesicles (Nath et al. 2007). Therefore, we hypothesize that *lc*-KIFC1 was not limited to testis but may also be involved diffusely in cargo transportation in different tissues, such as heart, liver, and kidney. Consequently, the
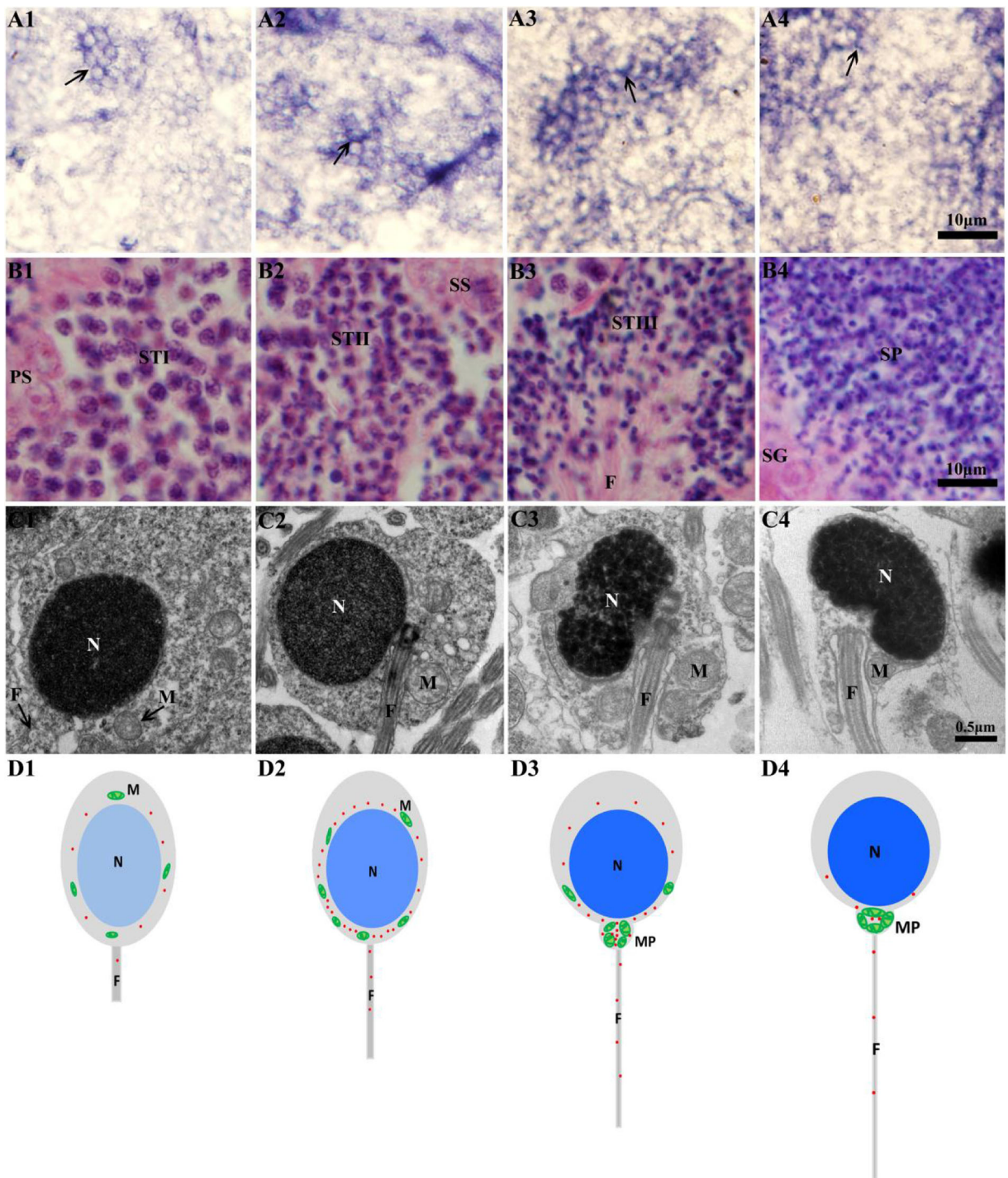
function of KIFC1 in various tissues in *L. crocea* needs to be further investigated. Furthermore, examination of different testis developmental growth stages in testis demonstrated that *lc-kifc1* mRNA expression gradually increased with continuous testis development before decreasing dramatically when testis maturation was reached. In stage II of development, the testes mainly contained spermatogonia and

◄ **Fig. 6** In situ hybridization of *lc-kifc1* mRNA expression and structural characteristics of spermatid during the *Larimichthys crocea* spermiogenesis. **a1–a4** show the results of in situ hybridization. **b1–b4** show the histological results through H.E. staining. **c1–c4** show the ultrastructural results. **d1–d4** show the schematic diagrams. **a1, b1, c1, –d1** Early stage of spermiogenesis. These figures show that the nucleus was round or oblong (**b1**) and mitochondria were randomly distributed in the cytoplasm (**c1**, *arrow*). The *kifc1* mRNA signals (**a1**, *arrows blue signal*; **d1**, *red dots*) were weakly distributed around the nuclear membrane. **a2, b2, c2, d2** Middle stage of spermiogenesis. These figures show that the nucleus was round and slightly smaller in size (**b2**) and mitochondria began to migrate toward one end of the nucleus (**c2**). The *kifc1* mRNA signals (**a2**, *arrows blue signal*; **d2**, *red dots*) were increased compared to the early stage and concentrated on cytoplasm and the side of the nucleus where the flagellum has been formed (**c2**). **a3, b3, c3, d3** Late stage of spermiogenesis. These figures show that the nucleus underwent enormous morphological change, in which process the nucleus gradually became condensed (**b3, c3**) and mitochondria migrated to the bottom of the nucleus forming the midpiece (**d3**). The *kifc1* mRNA signals (**a3**, *arrows blue signal*; **d3**, *red dots*) were strongly assembled at the one end of the nucleus. **a4, b4, c4, d4** Mature sperm. These figures show that *kifc1* mRNA signals (**a4**, *arrows blue signal*; **d4**, *red dots*) were weakly appeared at the tail but, in general, were dramatically decreased compared to other stages of spermiogenesis. *N* nucleus, *M* mitochondria, *F* flagellum, *SG* spermatogonia, *PS* primary spermatocyte, *SS* secondary spermatocyte, *ST* spermatid, *SP* spermatozoon

Fig. 7 Specificity test of the primary antibody by western blotting. *Lane M*: protein markers; *lane Anti-KIFC1*: the specific band visualized by chemical luminescence detection via X-ray

primary spermatocytes, and some of them contained secondary spermatocytes. In this stage, the expression of *lc-kifc1* mRNA was the lowest. When testis development advanced to the III stage, a small amount of spermatids began to appear and *lc-kifc1* mRNA expression quantity began to rise. In stage IV of testis development, there appeared a large number of spermatids, and the expression of *lc-kifc1* mRNA reached its peak at this time. Finally, when the testis entered into stage V of maturation, the testis was almost full of spermatozoa, and the expression of *lc-kifc1* mRNA decreased drastically. This result suggests that when spermatids began to undergo dramatic morphological changes, KIFC1 started to play an important role, and KIFC1 ceased to perform the task until a series of changes were complete. These results may indicate that KIFC1 is closely related to spermiogenesis in *L. crocea*.

The spatial and temporal distribution pattern of *lc-kifc1* mRNA during spermiogenesis

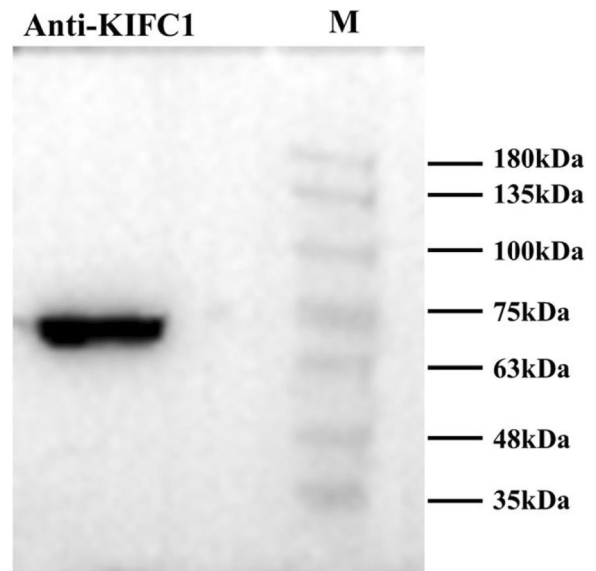A detailed spatial and temporal distribution pattern of *lc-kifc1* mRNA provided important information

regarding the time and site of expression of this motor protein during *L. crocea* spermiogenesis, thereby offering further insight on the mechanisms of the motor protein functions. In situ hybridization (ISH) has made it possible to directly observe the distribution of mRNA in spermatogenic cells (Zou et al. 2002). The results suggest that *lc-kifc1* mRNA expression was closely associated with nucleus reshaping and flagellum formation in multifarious developmental spermatids. In the early spermatids, *lc-kifc1* mRNA signals were weakly distributed in the cytoplasm. This may be because in this stage, morphological differentiation has not yet begun and motor protein probably has not started to work. In the intermediate spermatids, its mRNA signals were increased compared to that of the early stage and located at the periphery of the nuclear membrane and the side of the nucleus. In the late spermatids, the expression of *lc-kifc1* mRNA was visibly strong and highly centralized at the one end of the nucleus. It can be seen that *lc-kifc1* mRNA signals rapidly increased in the period of nuclear shaping and flagellum formation, which implies a key role of *kifc1* in these processes. In mature sperm, the expression *lc-kifc1* was decreased to a level lower than that of the other stages. This may provide more evidence for the role of *kifc1* in major cytological changes.
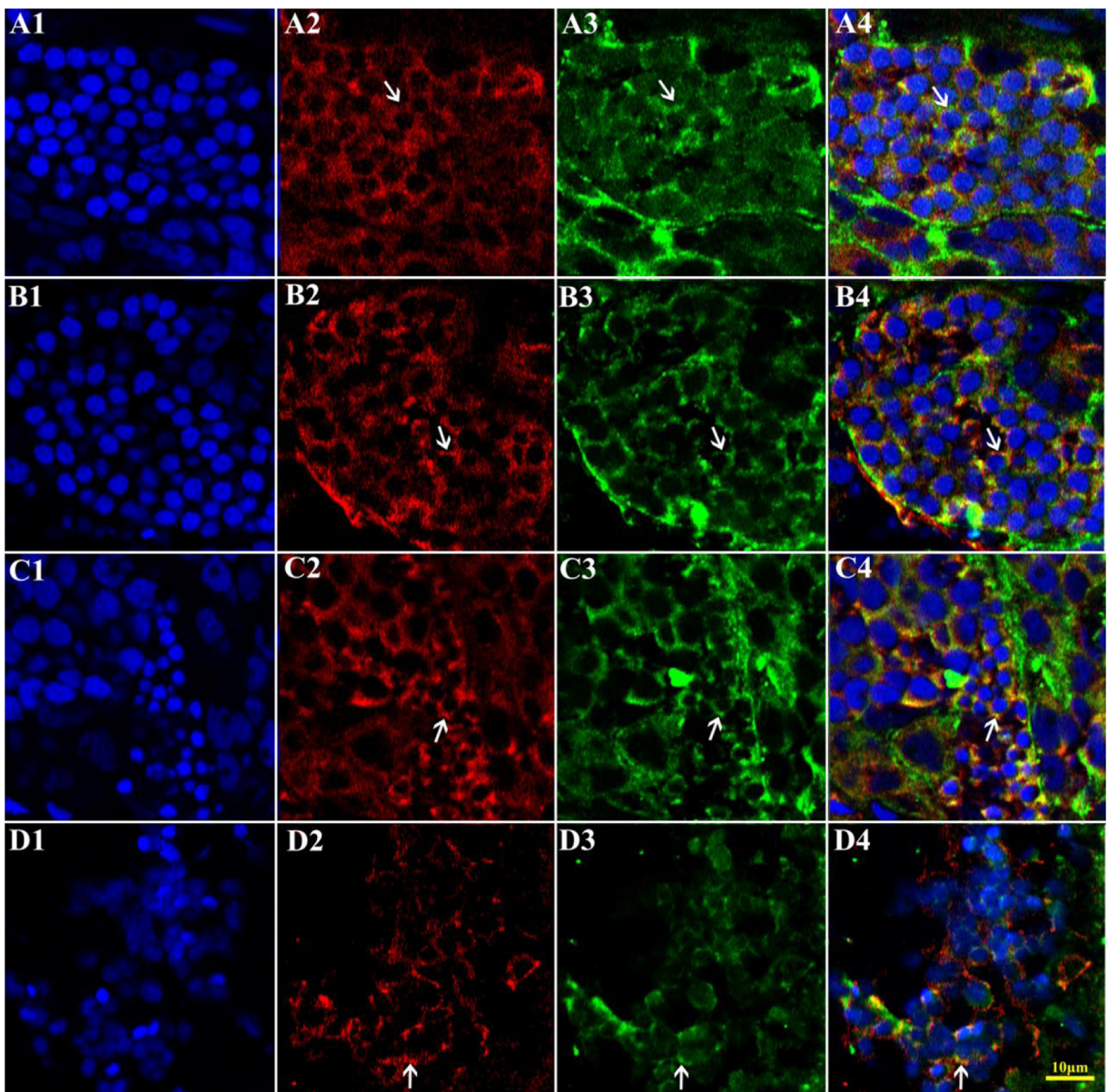
Fig. 8 Immunofluorescent localization of tubulin and KIFC1 during the *L. crocea* spermiogenesis. **a1**, **b1**, **c1**, **d1** DAPI nuclear staining (*blue staining*). **a2**, **b2**, **c2**, **d2** Tubulin staining (*red staining*). **a3**, **b3**, **c3**, **d3** KIFC1staining (*green staining*). **a4**, **b4**, **c4**, **d4** Merged immunofluorescent images. **a1–a4** Early stage of spermiogenesis. These figures show that tubulin and KIFC1 were co-localized in the cytoplasm and near the nuclear membrane. **b1**– **b4** Middle stage of spermiogenesis. These figures show that tubulin and KIFC1 were strongly co-localized in the cytoplasm and at the side of the nucleus. **c1–c4** Late stage of spermiogenesis. These figures show that tubulin and KIFC1 were mainly co-localized in the one end of the nucleus. **d1–d4** Mature sperm. These figures show that tubulin and KIFC1 were weakly co-localized in the bottom of the nucleus

The cargo of KIFC1 during spermiogenesis of *L. crocea*

Subsequently, colocalization of KIFC1 and tubulin was performed to further explore the role of KIFC1 in cellular transformations during spermiogenesis of

L. crocea. Microtubules are composed of tubulin, the concentrated signals of tubulin on behalf of the microtubules. At the early spermatids, the protein was expressed marginally, and the microtubules were aligned in an orderly fashion around the nucleus.
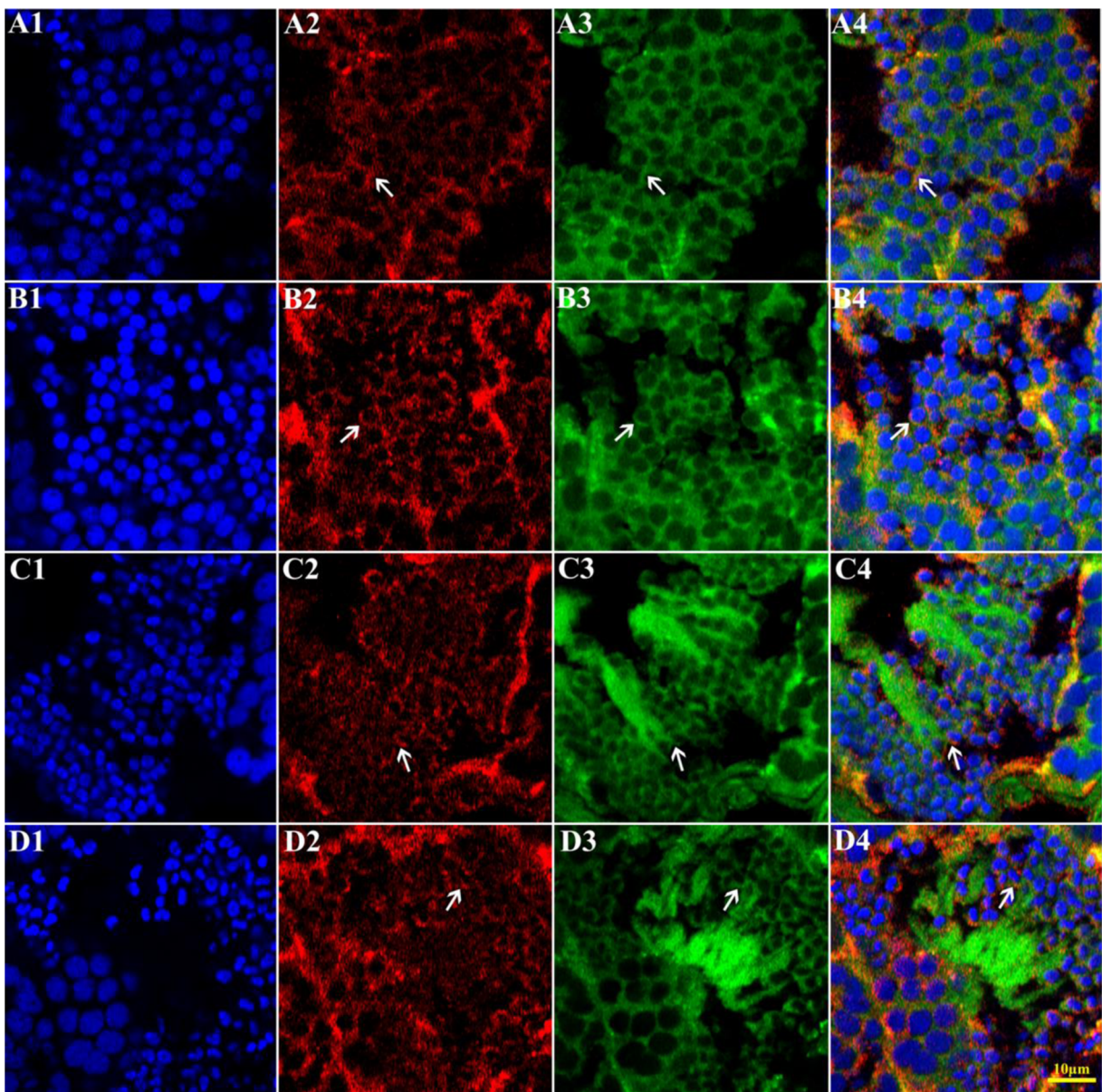
Fig. 9 Immunofluorescent localization of KIFC1 and MitoTracker (mitochondria) during *Larimichthys crocea* spermiogenesis. **a1**, **b1**, **c1**, **d1** DAPI nuclear staining (*blue staining*). **a2**, **b2**, **c2**, **d2** KIFC1staining (*red staining*). **a3**, **b3**, **c3**, **d3** MitoTracker staining (*green staining*). **a4**, **b4**, **c4**, **d4** Merged immunofluorescent images. **a1**–**a4** Early stage of spermiogenesis. These figures show that KIFC1 and MitoTracker were co-localized in the cytoplasm and near the nuclear membrane. **b1**–**b4** Middle stage of spermiogenesis. These figures show that KIFC1 and MitoTracker were abundantly co-localized in the cytoplasm and at the side of the nucleus. **c1**–**c4** Late stage of spermiogenesis. These figures show that KIFC1 and MitoTracker were primarily co-localized at the one end of the nucleus as part of the midpiece. **d1**–**d4** Mature sperm. These figures show that KIFC1 and MitoTracker were slightly co-localized in the midpiece and flagellum of the tail

When it comes to the middle spermatids, the protein began to be expressed and mainly co-localize with cytoplasmic microtubules. Similarly, in late spermatids where pronounced nuclear condensation and deformation took place and the midpiece of flagellum began to form which was present in side of the nucleus, expression of the protein was maintained at a high level and most protein signals were detected to

one end of the nucleus and overlapped with perinuclear microtubules. We also used immunofluorescence (IF) to locate of mitochondria in order to identify the protein transport substrates involved in midpiece formation. In early spermatids, Mito-Tracker was equably distributed around the nucleus. However, with the formation of midpiece, the Mito-Tracker was almost gathered in a point of the spermatids, when the flagellum formed position in late spermatids. Moreover, combining with the IF of KIFC1 and tubulin, the signals of Mito-Tracker had part overlapped position with them. These results were in agreement with our previous studies that KIFC1 is essential for the shaping of the sperm nucleus in *Octopus tankahkeei* (Wang et al. 2010b, c) and it also participates in the formation of the flagellum through the transportation of the mitochondria in *Eumeces chinensis* (Hu et al. 2013). Based on these results, we delineate a model pattern for the location of KIFC1 during spermiogenesis of *L. crocea* (Fig. 10).

The importance of KIFC1 during nuclear reshaping and flagellum formation

From the ISH and IF experimental results of the distribution of KIFC1 in *L. crocea*, we can easily

surmise a relationship between dramatic changes of the nucleus and the expression of KIFC1, meaning that when the nucleus begins to transform, KIFC1 signals are increased to transport specific cargo to promote this reshaping. Upon development to mature sperm, KIFC1 expression decreases to its lowest level. During the transformation of the nucleus, there must be some related mechanisms responsible for this process. It has been proven that KIFC1 could interact with the manchette of a special microtubule structure and certain nuclear membrane components, like NUP62 and importin β, may be involved in the nuclear reshaping process in rats (Yang and Sperry 2003; Yang et al. 2006). In *Octopus tankahkeei*, KIFC1 actively participated in sperm nuclear morphogenesis, possibly by bridging the manchette-like perinuclear microtubules with the nucleus and aiding in the nucleocytoplasmic transportation of specific cargo (Wang et al. 2010b, c). Compared to the mammalian and cephalopod spermatid nuclear reshaping, we assume that the *L. crocea* spermatid nucleus undergoes a significant change during spermiogenesis and, in this process, some specific complexes and structures may be formed which play important functions. At present, there is no evidence for the presence of a manchette-like microtubule in *L. crocea* spermatids. Therefore, further research is required
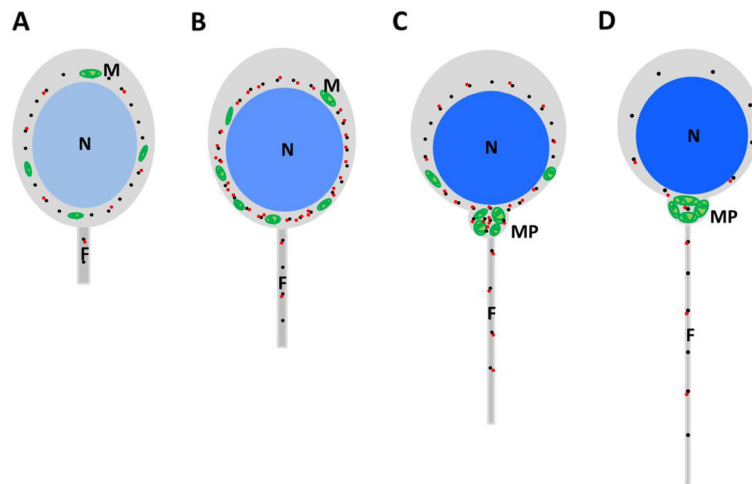
Fig. 10 A model scheme demonstrating the dynamic distribution of KIFC1 during spermiogenesis of *Larimichthys crocea*. The *black granule* represents the tubulin. The *red granule* represents the KIFC1 protein; its density corresponds to an abundance of protein signals. *Different shades* in nucleus represent the degree of chromatin condensation. **a** In early spermatid, the signal of KIFC1 is already appeared with a low level. **b** In middle spermatid, the

signal of KIFC1 is gradually increased as well as emerged in the cytoplasm and the side of the nucleus. **c** In late spermatid, the KIFC1 signals predominantly accumulate at the bottom of the nucleus to form midpiece structure. **d** In mature sperm, the KIFC1 signals are diminished but still appeared in the midpiece and flagellum of the tail. *N* nucleus, *M* mitochondria, *F* flagellum, *MP* midpiece

to determine whether a similar manchette structure is involved in facilitate nuclear shaping in conjunction with the motor protein KIFC1 in *L. crocea*. In addition, we also observed a phenomenon in spermatids with growing the flagella; the KIFC1 signal and Mito-Tracker are seen concentrated at the tail region together, indicating a possibility that the KIFC1 is responsible for the transport of mitochondria to the bottom of the nucleus and is actively involved in the formation of flagellum midpiece (Yang and Sperry 2003). Previous studies have shown that some types of kinesin are located in the sperm tail, either in the principal piece of the sperm tail or transported mitochondria in spermatid (Diefenbach et al. 1998; Zhang et al. 2004). The mitochondria are transferred from the cytoplasm to the membrane for the development of the midpiece and used either as carriers for structural materials or for the fixation of subcellular structures (Kotaja et al. 2004a). Recently, research has provided evidence that kinesin-II is localized in the midpiece and flagellum of *Octopus tannkahkeei* (Wang et al. 2010a) and *Cynops orientalis* (Hu et al. 2012) which as a key player in intraflagellar transport and is dispensable for the formation of cilia and flagella. We speculate that KIFC1 is likely to take part in the assembly and maintenance of spermatic flagellum and intraflagellar transport. Validation of this hypothesis requires the use of knockout or RNA interference and other technologies.

Conclusion

We have first described the existence of a *kifc1* homolog (*lc-kifc1*) gene in the testis of the *L. crocea*. Tissue expression analysis showed that *lc-kifc1* mRNA is expressed in all tissues examined, especially in the testis. The results of ISH and IF indicated that the motor protein KIFC1 contributes substantially to nucleus reshaping and flagellum formation during spermiogenesis. This research is of great significance for reconstruction of evolutionary lines at a molecular level; it provides new clues for understanding the functions of kinesin motors during spermiogenesis in the teleost. However, the mechanisms, including the targeting of specific cargo and regulation of cargo binding, transport, and release by the *kifc1* gene, remain unclear. Further

duplication and validation studies are needed to clarify these current findings.

Compliance with ethical standards

Conflict of interest The authors declare no conflict of interest.

References

Bernasconi P, Cappelletti C, Navone F, Nessi V, Baggi F, Vernos I, Romaggi S, Confalonieri P, Mora M, Morandi L, Mantegazza R (2008) The kinesin superfamily motor protein KIF4 is associated with immune cell activation in idiopathic inflammatory myopathies. J Neuropathol Exp Neurol 67(6): 624–632

Cai S, Weaver LN, Ems-McClung SC, Walczak CE (2009) Kinesin-14 family proteins HSET/XCTK2 control spindle length by cross-linking and sliding microtubules. Mol Biol Cell 20:1348–1359

Diefenbach RJ, Mackay JP, Armati PJ, Cunningham AL (1998) The C-terminal region of the stalk domain of ubiquitous human kinesin heavy chain contains the binding site for kinesin light chain. Biochemistry 37:16663–16670

Ems-McClung SC, Zheng YX, Walczak CE (2004) Importin α/β and ran-GTP regulate XCTK2 microtubule binding through a bipartite nuclear localization signal. Mol Biol Cell 15:46–57

Endow SA, Chandra R, Komma DJ, Yamamoto AH, Salmon ED (1994) Mutants of the *Drosophila* NCD microtubule motor protein cause centrosomal and spindle pole defects in mitosis. J Cell Sci 107:859–867

Fawcett DW (1975) The mammalian spermatozoon. Dev Biol 44(2):394–436

Goshima G, Vale RD (2005) Cell cycle-dependent dynamics and regulation of mitotic kinesins in Drosophila S2 cells. Mol Biol Cell 16:3896–3907

He Z, Kokkinaki M, Dym M (2009) Signaling molecules and pathways regulating the fate of spermatogonial stem cells. Microsc Res Tech 72:586–595

Hermo L, Pelletier RM, Cyr DG, Smith CE (2010a) Surfing the wave, cycle, life history, and genes/proteins expressed by testicular germ cells. Part 1: background to spermatogenesis, spermatogonia, and spermatocytes. Microsc Res Tech 73: 241–278

Hermo L, Pelletier RM, Cyr DG, Smith CE (2010b) Surfing the wave, cycle, life history, and genes/proteins expressed by testicular germ cells. Part 2: changes in spermatid organelles associated with development of spermatozoa. Microsc Res Tech 73:279–319

Hess RA, Renato FL (2008) Spermatogenesis and cycle of the seminiferous epithelium. Adv Exp Med Biol 636:1–15

Hirokawa N, Noda Y (2008) Intracellular transport and kinesin superfamily proteins, KIFs: structure, function, and dynamics. Physiol Rev 88:1089–1118

Hirokawa N, Takemura R (2004) Kinesin superfamily proteins and their various functions and dynamics. Exp Cell Res 301:50–59

Hirokawa N, Noda Y, Tanaka Y, Niwa S (2009) Kinesin superfamily motor proteins and intracellular transport. Nat Rev Mol Cell Biol 10:682–696

Ho NY, Li VWT, Poon WL, Cheng SH (2008) Cloning and developmental expression of kinesin superfamily7 (kif7) in the brackish medaka (Oryzias melastigma), a close relative of the Japanese medaka (Oryzias latipes). Mar Pollut Bull 57:425–432

Hou CC, Yang WX (2013) Acroframosome-dependent KIFC1 facilitates acrosome formation during spermatogenesis in the caridean shrimp Exopalaemon modestus. PLoS One 8:e76065

Hu JR, Xu N, Tan FQ, Wang DH, Liu M, Yang WX (2012) Molecular characterization of a KIF3A-like kinesin gene in the testis of the Chinese fire-bellied newt Cynops orientalis. Mol Biol Rep 39:4207–4214

Hu JR, Liu M, Wang DH, Hu YJ, Tan FQ, Yang WX (2013) Molecular characterization and expression analysis of a KIFC1-like kinesin gene in the testis of Eumeces chinensis. Mol Biol Rep 40:6645–6655

Kikkawa M (2008) The role of microtubules in processive kinesin movement. Trends Cell Biol 18(3):128–135

Kimmins S, Kotaja N, Fienga G, Kolthur US, Brancorsini S, Hogeveen K, Monaco L, Sassone-Corsi P (2004) A specific programme of gene transcription in male germ cells. Reprod BioMed Online 8(5):496–500

Kotaja N, De Cesare D, Macho B, Monaco L, Brancorsini S, Goossens E, Tournaye H, Gansmuller A, Sassone-Corsi P (2004a) Abnormal sperm in mice with targeted deletion of the act (activator of cAMP-responsive element modulator in testis) gene. Proc Natl Acad Sci U S A 101:10620–10625

Lawrence CJ, Dawe RK, Christie KR et al (2004) A standardized kinesin nomenclature. J Cell Biol 167(1):19–22

Li Z, Pan CY, Zheng BH, Xiang L, Yang WX (2010) Immunocytochemical studies on the acroframosome during spermiogenesis of the caridean shrimp Macrobrachium nipponense (Crustacea, Natantia). Invertebr Reprod Dev 54(3):121–131

Lui WY, Cheng CY (2008) Transcription regulation in spermatogenesis. Adv Exp Med Biol 636:115–132

Miki H, Setou M, Kaneshiro K, Hirokawa N (2001) All kinesin superfamily protein, KIF, genes in mouse and human. Proc Natl Acad Sci U S A 98:7004–7011

Miki H, Okada Y, Hirokawa N (2005) Analysis of the kinesin superfamily: insights into structure and function. Trends Cell Biol 15:467–476

Mountain V, Simerly C, Howard L, Ando A, Schatten G et al (1999) The kinesin-related protein, HSET, opposes the activity of Eg5 and cross-links microtubules in the mammalian mitotic spindle. J Cell Biol 147:351–365

Mukhopadhyay A, Nieves E, Che FY, Wang J, Jin LJ, Murray JW, Gordon K, Angeletti RH, Wolkoff AW (2011) Proteomic analysis of endocytic vesicles: Rab1a regulates motility of early endocytic vesicles. J Cell Sci 124(5):765–775

Nath S, Bananis E, Sarkar S, Stockert RJ, Sperry AO, Murray JW, Wolkoff AW (2007) Kif5B and Kifc1 interact and are required for motility and fission of early endocytic vesicles in mouse liver. Mol Biol Cell 18(5):1839–1849

Navolanic PM, Sperry AO (2000) Identification of isoforms of a mitotic motor in mammalian spermatogenesis. Biol Reprod 62:1360–1369

Noda Y, Sato-Yoshitake R, Kondo S, Nangaku M, Hirokawa N (1995) KIF2 is a new microtubule-based anterograde motor that transports membranous organelles distinct from those carried by kinesin heavy chain or KIF3A/B. J Cell Biol 129:157–167

Noda Y, Okada Y, Saito N, Setou M, Xu Y, Zhang Z, Hirokawa N (2001) KIFC3, a microtubule minus end-directed motor for the apical transport of annexin XIIIb-associated Triton-insoluble membranes. J Cell Biol 155:77–88

Oakberg EF (1956) A description of spermiogenesis in the mouse and its use in analysis of the cycle of the seminiferous epithelium and germ cell renewal. Am J Anat 99:391–413

Saito N, Okada Y, Noda Y, Kinoshita Y, Kondo S, Hirokawa N (1997) KIFC2 is a novel neuron-specific C-terminal type kinesin superfamily motor for dendritic transport of multivesicular body-like organelles. Neuron 18:425–438

Sperry AO, Zhao LP (1996) Kinesin-related proteins in the mammalian testes: candidate motors for meiosis and morphogenesis. Mol Biol Cell 7:289–305

Tan FQ, Ma XX, Zhu JQ, Yang WX (2013) The expression pattern of the C-terminal kinesin gene kifc1 during the spermatogenesis of Sepiella maindroni. Gene 532:53–62

Vale RD (2003) The molecular motor toolbox for intracellular transport. Cell 112:467–480

Walczak CE, Verma S, Mitchison TJ (1997) XCTK2: a kinesinrelated protein that promotes mitotic spindle assembly in Xenopus laevis egg extracts. J Cell Biol 136(4):859–870

Wang R, Sperry AO (2008) Identification of a novel leucine-rich repeat protein and candidate PP1 regulatory subunit expressed in developing spermatids. BMC Cell Biol 9:9

Wang W, Dang R, Zhu JQ, Yang WX (2010a) Identification and dynamic transcription of KIF3A homologue gene in spermiogenesis of octopus tankahkeei. Comp Biochem Physiol 157:237–245

Wang W, Zhu JQ, Yang WX (2010b) Molecular cloning and characterization of KIFC1-like kinesin gene (ot-kifc1) from Octopus tankahkeei. Comp Biochem Physiol 156:174–182

Wang W, Zhu JQ, Yu HM, Tan FQ, Yang WX (2010c) KIFC1-like motor protein associates with the cephalopod manchette and participates in sperm nuclear morphogenesis in Octopus tankahkeei. PLoS One 5:e15616

Wang YT, Mao H, Hou CC, Sun X, Wang DH, Zhou H, Yang WX (2012) Characterization and expression pattern of KIFC1-like kinesin gene in the testis of the Macrobrachium nipponense with discussion of its relationship with structure lamellar complex (LCx) and acroframosome (AFS). Mol Biol Rep 39(7):7591–7598

Xu Y, Takeda S, Nakata T, Noda Y, Tanaka Y, Hirokawa N (2002) Role of KIFC3 motor protein in Golgi positioning and integration. J Cell Biol 158:293–303

Yang WX, Sperry AO (2003) C-terminal kinesin motor KIFC1 participates in acrosome biogenesis and vesicle transport. Biol Reprod 69:1719–1729

Yang WX, Jefferson H, Sperry AO (2006) The molecular motor KIFC1 associates with a complex containing nucleoporin NUP62 that is regulated during development and by the small GTPase RAN. Biol Reprod 74:684–690

Yu KM, Hou L, Zhu JQ, Ying XP, Yang WX (2009) KIFC1 participates in acrosomal biogenesis, with discussion of its importance for the perforatorium in the Chinese mitten crab *Eriocheir sinensis*. Cell Tissue Res 337:113–123

Zhang Y, Sperry AO (2004) Comparative analysis of two C-terminal kinesin motor proteins: KIFC1 and KIFC5A. Cell Motil Cytoskel 58:213–230

Zhang Y, Oko R, van der Hoorn FA (2004) Rat kinesin light chain 3 associates with spermatid mitochondria. Dev Biol 275:23–33

Zhu CJ, Zhao J, Bibikova M, Leverson JD, Wetzel EB, Fan JB, Abraham RT, Jiang W (2005) Functional analysis of human microtubule-based motor proteins, the kinesins and dyneins, in mitosis/cytokinesis using RNA interference. Mol Biol Cell 16(7):3187–3199

Zou Y, Millette CF, Sperry AO (2002) KRP3A and KRP3B: candidate motors in spermatid maturation in the seminiferous epithelium. Biol Reprod 66:843–855